Effect of underlying boron nitride thickness on photocurrent response in molybdenum disulfide - boron nitride heterostructures

Milinda Wasala, Jie Zhang, Sujoy Ghosh, Baleeswaraiah Muchharla, Rachel Malecek, Dipanjan Mazumdar, Hassana Samassekou, Moses Gaither-Ganim, and Andrew Morrison
Department of Physics, Southern Illinois University Carbondale, Carbondale, Illinois 62901, USA

Nestor-Perera Lopez, Victor Carozo, and Zhong Lin
Department of Physics and Center for 2-Dimensional and Layered Materials, The Pennsylvania State University, University Park, Pennsylvania 16802, USA

Mauricio Terrones
Department of Physics and Center for 2-Dimensional and Layered Materials, The Pennsylvania State University, University Park, Pennsylvania 16802, USA; and Department of Chemistry and Department of Materials Science and Engineering, The Pennsylvania State University, University Park, Pennsylvania 16802, USA

Saikat Talapatra[a)]
Department of Physics, Southern Illinois University Carbondale, Carbondale, Illinois 62901, USA

(Received 11 September 2015; accepted 17 November 2015)

Here we report on the photocurrent response of two-dimensional (2D) heterostructures of sputtered MoS_2 on boron nitride (BN) deposited on (001)-oriented Si substrates. The steady state photocurrent (I_{ph}) measurements used a continuous laser of $\lambda = 658$ nm ($E = 1.88$ eV) over a broad range of laser intensities, P ($\sim 1\ \mu W < P < 10\ \mu W$), and indicate that I_{ph} obtained from MoS_2 layers with the 80 nm BN under layer was ~4 times higher than that obtained from MoS_2 layers with the 30 nm BN under layer. We also found super linear dependence of I_{ph} on P ($I_{ph} \propto P^{\gamma}$, with $\gamma > 1$) in both the samples. The responsivities obtained over the range of laser intensity studied were in the order of mA/W (~12 and ~2.7 mA/W with 80 nm BN and 30 nm BN under layers, respectively). These investigations provide crucial insight into the optical activity of MoS_2 on BN, which could be useful for developing a variety of optoelectronic applications with MoS_2 or other 2D transition metal dichalcogenide heterostructures.

I. INTRODUCTION

Two-dimensional (2D) crystals and layered transition metal dichalcogenide (TMDC) systems, in recent times, have gained significant attention due to the virtue of their extraordinary properties, specifically related to light matter interaction.[1–4] Molybdenum disulphide (MoS_2), similar to several other TMDC semiconductors, has attracted substantial interest due to its special properties that might lead to several photonics based applications.[5–11] The presence of a direct band gap in single layer MoS_2 and the observation of strong photoluminescence is, to date, lauded as some of the most fascinating properties of this material. Investigations on other members of the TMDC family, for example, $MoSe_2$, WS_2, WSe_2, $InSe_2$, etc., indicate that one to a few layers of 2D-TMDCs can play a crucial role in applications related to optoelectronics ranging from fast photo-switches to solar cells. With a range of investigations pointing toward the possible potential of these materials for future applications, it is slowly becoming clear that some of the niche properties of TMDC materials also depend on a variety of other factors such as, the dielectric environment, the nature of the supporting substrates, etc. For example, in one of the initial studies, it was shown that multilayer MoS_2 field effect transistors (FETs) on SiO_2 mostly exhibited unipolar, n-type behavior with mobilities ~30–60 cm^2/V s, independent of the SiO_2 thickness. However, multilayer MoS_2 FETs fabricated on polymer substrates, such as polymethyl methacrylate, exhibited ambipolar behavior with electron and hole mobilities reaching ~480 cm^2/V s in relation to increasing polymer thickness.[12]

Such a behavior, as several other investigations have indicated, is not restricted only to electronic properties, but also extends to other important physical properties as well. It was recently shown that the vibrational properties of MoS_2 crystals grown (using sulfurization of MoO_2) on SiO_2 substrates are quite different from those that were grown on quartz substrates.[13] One of the initial studies in this field revealed that the Raman and photoluminescence

Contributing Editor: Joshua Robinson
[a)]Address all correspondence to this author.
e-mail: stalapatra@physics.siu.edu
DOI: 10.1557/jmr.2015.364

(PL) emission from single-layer MoS_2 depends significantly on the underlying substrate. In this study a variety of underlying dielectric and conducting substrates were used and it was shown that the absorption as well as emission properties of monolayer MoS_2 are strongly modulated by interference effects within different substrates.[14] On similar grounds, it was recently shown that it is extremely simple to control the photonic and electronic properties of thin layer tungsten selenide (WSe_2) by controlling the thickness of the underlying substrate.[15] Thus it is clear that the properties of a few atomic layers of 2D TMDCs are greatly affected by the underlying substrate as well as their heterostructures. Now tremendous effort is being devoted to create and characterize a variety of heterostructures using 2D layered TMDCs. For example, the growth and exotic properties of heterostructures involving WS_2/MoS_2, graphene/hexagonal boron nitride (BN), MoS_2/graphene, WS_2/BN, etc. are already demonstrated.[16–20]

Understanding substrate specific interactions and their effect on the structure and properties of 2D layered semiconductors and their heterostructures, is therefore, becoming essential to develop them for future functional applications. In this article, we report on the photoresponse studies of MoS_2–BN heterostructures grown on (001)-oriented Si substrates. We investigated vertical heterostructures consisting of ~20 nm of MoS_2 deposited on BN layers of a thickness of ~35 and ~80 nm (using precalibrated values). These samples will be classified as $20MoS_2$/35BN and $20MoS_2$/80BN from now on. We found that upon illuminating the devices using a continuous laser of $\lambda = 658$ nm ($E = 1.88$ eV) with a scaled laser intensity $P \sim 10$ μW, under high vacuum, the steady state photocurrent (I_{ph}) of $20MoS_2$/80BN samples was found to be ~120 nA, which was 4 times more than the values obtained from $20MoS_2$/35BN samples. The variation of I_{ph} on P was found to be super linear ($I_{ph} \propto P^{\gamma}$) with $\gamma = 1.04$ in $20MoS_2$/35BN and $\gamma = 1.07$ in $20MoS_2$/80BN over the whole range of laser intensities studied ($\sim 1\ \mu W < P < 10\ \mu W$). Within the same range of intensities, the responsivity values obtained for $20MoS_2$/80BN ~12 mA/W was an order of magnitude higher than the $20MoS_2$/35BN. We further investigated several devices fabricated from the sample with higher responsivity values ($20MoS_2$/80BN) under ambient conditions with the same laser source and at $P = 10$ μW. Under ambient conditions the value of responsivity was found to be substantially smaller (~1 mA/W) for these devices. A detailed discussion pertaining to the photocurrent behaviors seen in our experiments is also presented.

II. MATERIALS AND METHODS

Large area MoS_2–BN heterostructures were grown on (001)-oriented Si substrates with radio frequency (RF) magnetron sputtering using a multi-target AJA-300 high vacuum sputter deposition system (base pressure ~5×10^{-8} Torr) (AJA International, North Scituate, Massachusetts). Commercially available MoS_2 (99.95% purity) and BN (99.9%) were used. Argon was used as the process gas for the MoS_2 layer, while an Ar:N_2 (5:1) mixture was preferred for the BN layer. Both layers were deposited at 350 °C.

The layered heterostructure calibration and detailed structural analysis were performed using an x-ray reflectivity (XRR) technique (Phillips MRD, PANalytical, Boulder, Colorado) with a Cu K_α-source. Fitting to the XRR data was performed using the GenX software.[21]

Micro-Raman spectroscopy analysis of the samples grown by the sputter deposition of MoS_2 films on SiO_2 and BN substrates was performed utilizing a Renishaw inVia confocal microscope-based Raman spectrometer (Renishaw, Hoffman Estates, Illinois) using a 514.5 nm excitation wave length. Raman spectroscopic characterization was performed under ambient conditions with a backscattering geometry. The laser power was kept below 1.5 mW to prevent the damage on the samples. The laser spot size was maintained about 2 μm utilizing a 50× objective lens.

For performing electrical and photocurrent measurements, Chromium (Cr)/Gold (Au) (20 nm Cr/100 nm Au) contact pads were deposited on MoS_2/BN heterostructures using thermal evaporation of these metals through a shadow mask [transmission electron microscope (TEM) grid]. The samples were then mounted on a chip holder inside a close cycle helium cryostat with an optical window and the system was pumped down to a high vacuum level (~10^{-6} Torr) before performing the electrical and optical measurements. Current–voltage (I–V) measurements were performed using Keithley source meters (2400 series; Keithley Instruments Inc., Cleveland, Ohio) and the photo-response properties of these samples were investigated using a continuous wave solid-state laser system [wave length $\lambda = 658$ nm ($E = 1.88$ eV)].

III. RESULTS AND DISCUSSION

Results of structural characterization of one of the heterostructures, $20MoS_2$/35BN, are presented in Fig. 1. The XRR reflectivity curve of this sample is shown (solid black). We would like to note that for quantitative roughness estimation we have utilized XRR for the following reasons. XRR is one of the widely used techniques for providing roughness information for a large area specimen quickly, which typically is not possible using atomic force microscopy (AFM) or scanning electron microscopy (SEM). Further, interface roughness can also be characterized using XRR, which is a major advantage compared to both AFM and SEM.

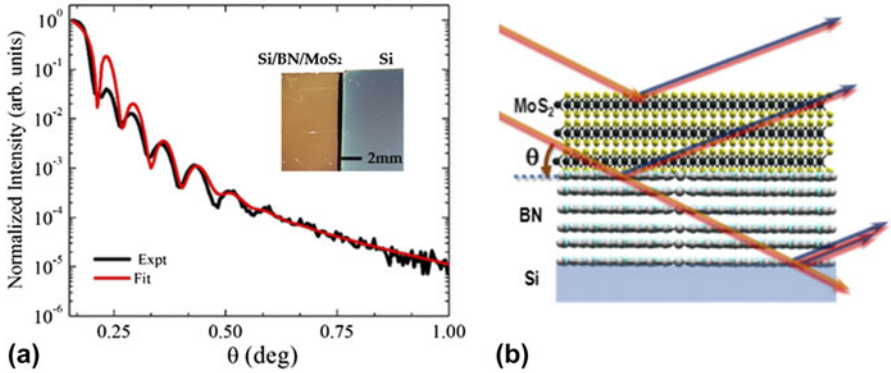

FIG. 1. (a) XRR data of the 20MoS_2/35BN sample, showing XRR fringes indicative of the presence of sharp interfaces in these heterostructures. The inset shows the optical image of the deposited 20MoS_2/35BN heterostructure and blank Si substrate. (b) Possible existence of these interfaces.

TABLE I. Parameters extracted from XRR reflectivity measurements are listed.

	MoS_2		BN		BN/Si interface	
Samples	Thickness (nm)	Roughness (nm)	Thickness (nm)	Roughness (nm)	Thickness (nm)	Roughness (nm)
20MoS_2/35BN	21.3	±3.8	25.8	±4.3	4.9	±3.2
20MoS_2/80BN	18.8	±5.6	82.4	±5.9	6.0	±4.9

Clear XRR fringes are observed in the data, which indicates that these multi-layers have reasonably sharp interfaces. A fit analysis of these data was performed to extract the thickness, roughness, and density of all the constituent layers (red curve). Apart from BN and MoS_2 layers, we found evidence of a rough, chemically mixed layer at the Si–BN interface in the samples. Without considering the existence of these layers, the goodness-of-fit was much higher than desirable. Even though the chemical composition of these layers cannot be quantified through this analysis, the fit density and scattering factor value are consistent with an oxy-nitride layer of Si and B at the Si–BN interface. This is not surprising since a native oxide layer of Si, and the presence of N_2 during BN deposition accentuates the nitride phase. The values of thickness and roughness of these interfacial layers obtained from our XRR investigations for both samples are provided in Table I. Apart from the presence of these interfacial layers, we also find a lower MoS_2 average density (compared to the bulk value) and small deviations from the nominal 1:2 MoS_2 stoichiometry within the sample area. However, Raman spectroscopy measurements performed on our samples showed clear evidence that the MoS_2 phase was present.

Raman spectroscopic investigations are routinely used to identify layered MoS_2 structures.[22–25] The data from the Raman measurements performed on 20MoS_2/35BN and 20MoS_2/80BN heterostructures are shown in Figs. 2(a) and 2(b), respectively. Multiple Raman spectra, with a laser exposure time of ~120 s, were collected from several areas of the samples to validate the reproducibility of the data as well as the uniformity of the deposited samples. The Raman spectra showed signatures of vibrational modes related to MoS_2. Two of the most prominent peaks, around 381 and 407 cm^{-1}, were observed in the Raman data for both the samples and can be, respectively, assigned to the first-order E^1_{2g} and A_{1g} modes at the Γ-point of the hexagonal Brillouin zone of 2D-MoS_2.[11,13,22–25] A broad peak around 450 cm^{-1} was also observed, which could be due to the second order longitudinal acoustic phonons near the *M*-point of the Brillouin zone [2LA(M)], often observed in multiple layers of MoS_2. Further, a sharp peak, around 285 cm^{-1}, was observed [see the inset of Figs. 2(a) and 2(b)]. This peak is generally associated with E_{1g} phonons near the Γ-point and was recently observed in multilayer samples grown using direct vapor-phase sulfurization of MoO_2 on SiO_2/Si as well as quartz substrates.[13]

We next investigated the photo-current response properties of the MoS_2/BN heterostructures. Before performing the photo-switching experiments, current–voltage (*I–V*) characteristics of these devices were measured in a two probe configuration. The samples were between the two contact electrodes, biased up to ±1 V, for performing the *I–V* measurements. Figure 3(a) shows the *I–V* curves obtained from typical heterostructures (without any light illumination). *I–V* curves for both the structures were found to be linear in nature. This indicated that good ohmic contacts persisted between the MoS_2 channel and the metal electrodes within the applied voltage regime. The linearity of *I–V* curves without illumination was tested to show that within the applied voltage regime,

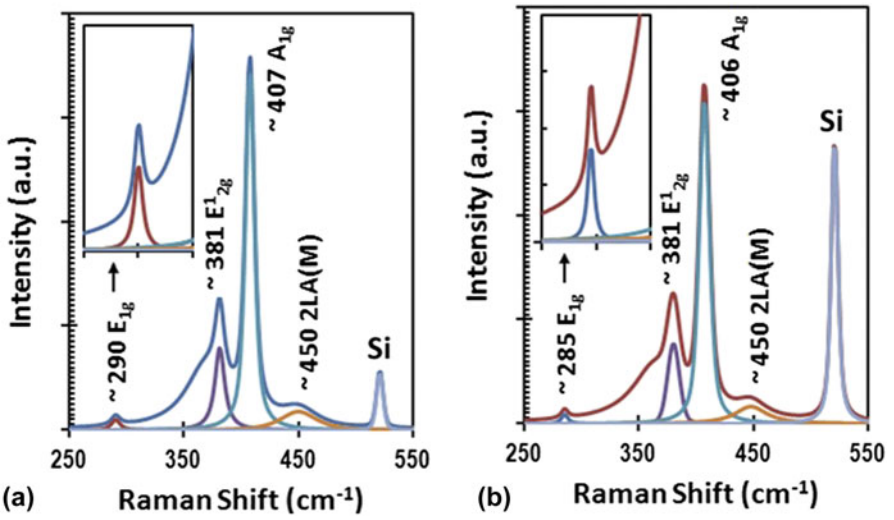

FIG. 2. (a) Raman spectrum obtained from the $20MoS_2/35BN$ sample. Several vibrational modes akin to MoS_2 layers are identified in this spectrum. The inset shows the presence of E_{1g} mode ~290 cm^{-1} in these samples. (b) The Raman spectrum obtained from the $20MoS_2/80BN$ sample. The inset shows the presence of E_{1g} mode ~285 cm^{-1} in these samples. The peak observed at 520 cm^{-1} in both these spectra belongs to the Si substrate on which these heterostructures were fabricated.

under which the measurements were performed, the contacts were able to replenish the carriers when they are drawn out from the material under an applied electric field. We found that the channel current is slightly increased with the increase in the thickness of the bottom BN layer.

In Figs. 3(b) and 3(c), the photo-switching characteristics of MoS_2/BN heterostructures at different laser intensities are shown. A source–drain voltage of 1 V was applied between the electrodes of the devices being measured and the laser intensity was varied from ~1 to 10 μW (scaled value of laser power according to the device area). The photo-switching measurements were performed in the following way. The device was continuously biased with 1 V without turning the laser ON and the current (I_{dark}) was recorded. Subsequently, the laser intensity was fixed at a specific power and was switched ON for about 10 s, during which the evolution of the current (I_{ill}) was recorded. This sequence was followed for the photo-response of these devices for several laser intensities. Between each "laser ON" sequence we waited until the channel current reached its initial I_{dark} value (about 20–30 s). The photo-current (I_{ph}) is the current obtained by subtracting the current under illumination from the current obtained under dark conditions at different laser intensities ($I_{ph} = I_{ill} - I_{dark}$).

In Fig. 3(d), dependence of I_{ph} on laser power (P) is presented. In this figure, I_{ph} as a function of P is plotted in a double logarithmic scale. The data obtained seems to fit very well with a power law dependence of the form $I_{ph} \propto P^{\gamma}$, where $\gamma = 1.04$ and $\gamma = 1.07$ for $20MoS_2/35BN$ and $20MoS_2/80BN$ heterostructures, respectively. This behavior is surprisingly different from most of the studies reported so far in the literature. Typically, in highly crystalline materials, the value of $\gamma = 0.5$ corresponds to bimolecular processes, or $\gamma = 1$ corresponds to monomolecular processes.[26] These processes are often observed in semiconducting systems with few trap states. Power exponents with values of γ ranging between 0.5 and 1 ($0.5 < \gamma < 1.0$) are also very common in disordered semiconductors and in chalcogenide glasses.[26–30] In the absence of the photo-phenomenon arising from photo-gating artifacts, thermoelectric effects and so on, fractional dependence of the power exponent seen in a variety of systems was explained on the basis of a theoretical model which assumes an exponential distribution of trap states in the mid-gap state.[26] Such fractional distribution was recently observed for thin film photo-detectors fabricated using liquid phase exfoliated MoS_2 materials.[11]

However, a few reports on the super linearity of power exponent γ in several systems have been reported in the past.[31,32] Though to date a clear theoretical understanding of such a phenomenon is still lacking, a few have tried to explain it on the basis of the presence of recombination centers with different energies and capture cross-sections.[26] More recently, such super linear dependence of I_{ph} over a broad range of laser power was also observed in a variety of compositionally different MoS_2 and $MoSe_2$ systems[33] and was explained on the basis of a model, which considered the presence of three types of recombination centers in the samples studied. Whether a similar model can be applied to explain the behavior seen in our experiments or some other, more complicated, phenomenon is responsible for the super linearity of the γ observed in the MoS_2/BN

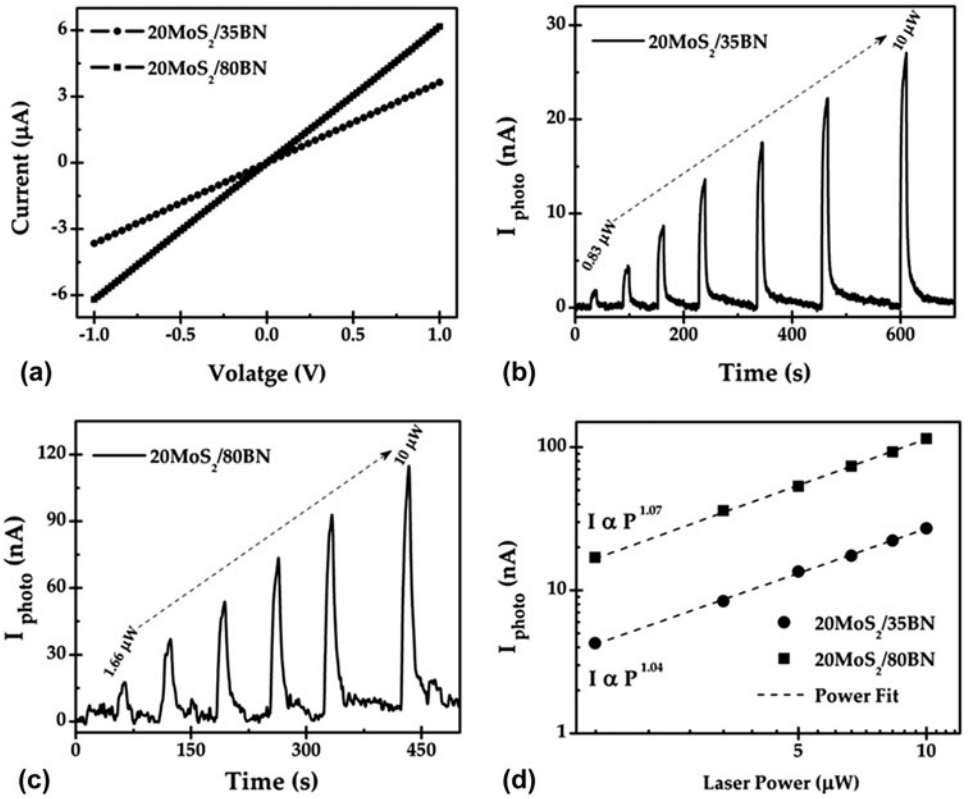

FIG. 3. (a) Linear current–voltage (*I–V*) response obtained from $20MoS_2/35BN$ and $20MoS_2/80BN$ samples is shown. (b) Room temperature photo-switching behavior of $20MoS_2/35BN$ under laser illumination of $\lambda = 658$ nm at different laser powers ~0.8–10 μW is shown. (c) Similar data, as shown in (b) are presented for $20MoS_2/80BN$. (d) Shows the variation of I_{ph} with laser intensity (at 10 μW) for both these samples. The dotted line in this figure indicates power fit to the data plotted on a double logarithmic scale. The measurements for all the data presented in this figure were performed at room temperature and under high vacuum ($\sim 10^{-6}$ Torr).

heterostructures, is, at present, beyond the scope of this article and will be investigated in greater detail in the future.

We also calculated the responsivity values of these samples at different laser powers. Responsivity (R) is defined as $R = I_{ph}/P_{light}$ (where P_{light} is the power of the incident light), and is an important performance factor used for quantifying the effectiveness of photoactive materials. Figure 4(a) shows the room temperature responsivity of the MoS_2/BN heterostructures measured under high vacuum ($\sim 10^{-6}$ Torr) at different laser powers. The responsivity at 10 μW was found to be ~2.7 and ~12 mA/W for $20MoS_2/35BN$ and $20MoS_2/80BN$ heterostructures, respectively. These responsivity values are several orders of magnitude greater than the responsivity of liquid exfoliated MoS_2 thin film photodetectors ~50 μA/W (Ref. 11) as well as chemical vapor deposition (CVD) grown multilayer WS_2 based devices ~22 μA/W.[27] Thus a very convincing evidence of the enhancement of photocurrent was observed with the increase in the underlying BN layer thickness in these heterostructure. Though, several factors can affect photocurrent generation in optically active semiconductors (e.g., presence of trap states), recent investigations show[14,15] that underlying dielectric layer has profound effects on the optical properties of TMDCs. For example, it was hypothesized[14,15] that due to the several layers present in these hetero-structures (e.g., MoS_2, BN, and Si) absorbed light can undergo multiple reflections between the layer boundaries. As a result of these multiple reflections, constructive interference between absorption and emission of light occurs. Such effects can substantially alter the optical properties of the top layer materials. We believe that a similar phenomenon is perhaps responsible in the present case as well.

We further found that the responsivity values for these heterostructures drastically reduce when they are exposed to ambient conditions. For example, the measurement on several $20MoS_2/80BN$ samples in the presence of air and with a laser illumination of 10 μW showed roughly an order of magnitude reduction in their responsivity (between 1 and 0.5 mA/W for five different devices measured) values. These results are presented in Fig. 4(b). Such reduction in responsivities is not surprising and is associated with the fact that MoS_2 surfaces are extremely sensitive to the surrounding environmental conditions.[34,35]

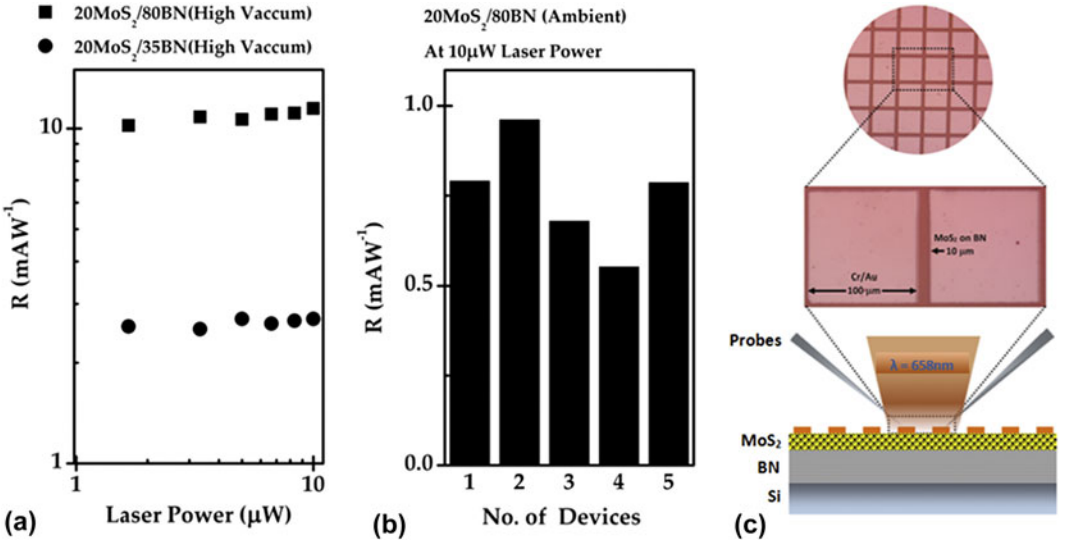

FIG. 4. (a) Responsivities obtained for the samples $20MoS_2/35BN$ and $20MoS_2/80BN$ as a function of laser power is shown. These measurements were performed at room temperature under a high vacuum of $\sim 10^{-6}$ Torr. (b) Responsivities obtained for five different $20MoS_2/80BN$ devices under ambient conditions. (c) Shows an optical micrograph of $20MoS_2/80BN$ with contact pads on top along with a schematic of the two point probe arrangement used for the measurements to obtain the data shown in (b).

Specifically, channel current in MoS_2 FETs deteriorates significantly under ambient conditions[34] as well as in the presence of oxygen.[35] Such deterioration is caused by the electron capturing nature of adsorbed oxygen on the sulfur or defect sites of MoS_2, which results in the reduction of the channel current.[34] We anticipate similar processes occurring in our case as well.

IV. CONCLUSION

We have shown that the thickness of BN layers significantly affects the photocurrent response properties of MoS_2 deposited on top of the layers. Our investigations show that an order of magnitude increase in photocurrents can be achieved in MoS_2 layers by simply increasing the underlying thickness of BN from 35 to 80 nm. We have also observed unusual super linear dependence of photocurrent in these heterostructures over the range of laser intensities studied. Further measurements with several other thicknesses of the BN under layer are underway and will be published subsequently. These future measurements are needed to conclusively understand the exact science behind the photocurrent response behavior observed in a MoS_2/BN system. Though our measurements specifically focused on MoS_2 on BN, we believe that such an outcome, in general, is possible for a variety of other optically active 2D TMDC layered heterostructures. However, the present study shows some encouraging results for creating functional heterostructures using the sputtering technique on Si. We believe that this method is also applicable for large area growth on any other substrates and can be, in principle, expanded to synthesize a layered 2D heterostructure on flexible substrates (e.g., thin polymer sheets, etc.) as well. Tuning of optical properties of TMDCs through substrate specific engineering, as reported here, is extremely valuable to develop 2D layered heterostructures for a variety of electronic and optoelectronic based future applications.

ACKNOWLEDGMENTS

This work is supported by the U.S. Army Research Office through a MURI Grant No. W911NF-11-1-0362. The X-ray reflectivity experiment shown was carried out in the Frederick Seitz Materials Research Laboratory Central Research Facilities, University of Illinois. D.M. would like to acknowledge Dr. Mauro Sardela for his help with X-ray measurements.

REFERENCES

1. K.S. Novoselov, D. Jiang, F. Schedin, T.J. Booth, V.V. Khotkevich, S.V. Morozov, and A.K. Geim: Two-dimensional atomic crystals. *Proc. Natl. Acad. Sci. U. S. A.* **102**, 10451 (2005).
2. D. Jariwala, V.K. Sangwan, L.J. Lauhon, T.J. Marks, and M.C. Hersam: Emerging device applications for semiconducting two-dimensional transition metal dichalcogenides. *ACS Nano* **8**, 1102 (2014).
3. N. Pradhan, D.A. Rhodes, S. Memaran, J.M. Poumirol, D. Smirnov, S. Talapatra, S. Feng, N. Perea-López, A.L. Elias, M. Terrones, P.M. Ajayan, and L. Balicas: Hall and field-effect mobilities in few layered p-WSe_2 field-effect transistors. *Sci. Rep.* **5**, 8979 (2015).
4. B. Radisavljevic, A. Radenovic, J. Brivio, V. Giacometti, and A. Kis: Single-layer MoS_2 transistors. *Nat. Nanotechnol.* **6**, 147 (2011).

5. S. Ghosh, S. Najmaei, S. Kar, R. Vajtai, N. Pradhan, J. Lou, L. Balicas, P.M. Ajayan, and S. Talapatra: Universal ac conductance in large area CVD grown MoS_2. *Phys. Rev. B* **89**, 125422 (2014).
6. Q.H. Wang, K. Kalantar-Zadeh, A. Kis, J.N. Coleman, and M.S. Strano: Electronics and optoelectronics of two-dimensional transition metal dichalcogenides. *Nat. Nanotechnol.* **7**, 699 (2012).
7. S. Kim, A. Konar, W. Hwang, J.H. Lee, J. Lee, J. Yang, C. Jung, H. Kim, J.B. Yoo, J.Y. Choi, Y.W. Jin, S.Y. Lee, D. Jena, W. Choi, and K. Kim: High-mobility and low-power thin-film transistors based on multilayer MoS_2 crystals. *Nat. Commun.* **3**, 1011 (2012).
8. Y. Zhang, J. Ye, Y. Matsuhashi, and Y. Iwasa: Ambipolar MoS_2 thin flake transistors. *Nano Lett.* **12**, 1136 (2012).
9. Z. Yin, H. Li, H. Li, L. Jiang, Y. Shi, Y. Sun, G. Lu, Q. Zhang, X. Chen, and H. Zhang: Single-layer MoS_2 phototransistors. *ACS Nano* **6**(1), 74 (2012).
10. H.S. Lee, S.W. Min, Y.G. Chang, M.K. Park, T. Nam, H. Kim, J.H. Kim, S. Ryu, and S. Im: MoS_2 nanosheet phototransistors with thickness-modulated optical energy gap. *Nano Lett.* **12**(7), 3695 (2012).
11. S. Ghosh, A. Winchester, B. Muchharla, M. Wasala, S. Feng, A.L. Elias, M.B.M. Krishna, T. Harada, C. Chin, K. Dani, S. Kar, M. Terrones, and S. Talapatra: Ultrafast intrinsic photoresponse and direct evidence of sub-gap states in liquid phase exfoliated MoS_2 thin films. *Sci. Rep.* **5**, 11272 (2015).
12. W. Bao, X. Cai, D. Kim, K. Sridhara, and M.S. Fuhrer: High mobility ambipolar MoS_2 field-effect transistors: Substrate and dielectric effects. *Appl. Phys. Lett.* **102**, 042104 (2013).
13. I. Bilgin, F. Liu, A. Vargas, A. Winchester, M.K.L. Man, M. Upmanyu, K. Dani, G. Gupta, S. Talapatra, A.D. Mohite, and S. Kar: Chemical vapor deposition synthesized atomically-thin molybdenum disulfide with optoelectronic-grade crystalline quality. *ACS Nano* **9**(9), 8822 (2015).
14. M. Buscema, G.A. Steele, H.S.J. van der Zant, and A. Castellanos-Gomez: The effect of the substrate on the Raman and photoluminescence emission of single-layer MoS_2. *Nano Res.* **7**, 561 (2014).
15. D-H. Lien, J.S. Kang, M. Amani, K. Chen, M. Tosun, H-P. Wang, T. Roy, M.S. Eggleston, M.C. Wu, M. Dubey, S-C. Lee, J-H. He, and A. Javey: Engineering light outcoupling in 2D materials. *Nano Lett.* **15**, 1356 (2015).
16. Y. Gong, J. Lin, X. Wang, G. Shi, S. Lei, Z. Lin, X. Zou, G. Ye, R. Vajtai, B.I. Yakobson, H. Terrones, M. Terrones, B.K. Tay, J. Lou, S.T. Pantelides, Z. Liu, W. Zhou, and P.M. Ajayan: Vertical and in-plane heterostructures from WS_2/MoS_2 monolayers. *Nat. Mater.* **13**, 1135 (2014).
17. Z. Liu, L. Song, S. Zhao, J. Huang, L. Ma, J. Zhang, J. Lou, and P.M. Ajayan: Direct growth of graphene/hexagonal boron nitride stacked layers. *Nano Lett.* **11**(5), 2032 (2011).
18. Y. Shi, W. Zhou, A.Y. Lu, W. Fang, Y.H. Lee, A.L. Hsu, S.M. Kim, K.K. Kim, H.Y. Yang, L.J. Li, J.C. Idrobo, and J. Kong: van der Waals epitaxy of MoS_2 layers using graphene as growth templates. *Nano Lett.* **12**(6), 2784 (2012).
19. M. Okada, T. Sawazaki, K. Watanabe, T. Taniguch, H. Hibino, H. Shinohara, and R. Kitaura: Direct chemical vapor deposition growth of WS_2 atomic layers on hexagonal boron nitride. *ACS Nano* **8**(8), 8273 (2014).
20. X. Zhang, F. Meng, J.R. Christianson, C. Arroyo-Torres, M.A. Lukowski, D. Liang, J.R. Schmidt, and S. Jin: Vertical heterostructures of layered metal chalcogenides by van der Waals epitaxy. *Nano Lett.* **14**(6), 3047 (2014).
21. M. Björck and G. Andersson: GenX: An extensible x-ray reflectivity refinement program utilizing differential evolution. *J. Appl. Cryst.* **40**, 1174 (2007).
22. B.C. Windom, W.G. Sawyer, and D.W. Hahn: A Raman spectroscopic study of MoS_2 and MoO_3: Applications to tribological systems. *Tribol. Lett.* **42**(3), 301 (2011).
23. H. Li, Q. Zhang, C.C.R. Yap, B.K. Tay, T.H.T. Edwin, A. Olivier, and D. Baillargeat: From bulk to monolayer MoS_2: Evolution of Raman scattering. *Adv. Funct. Mater.* **22**, 1385 (2012).
24. C. Lee, H. Yan, L.E. Brus, T.F. Heinz, J. Hone, and S. Ryu: Anomalous lattice vibrations of single- and few-layer MoS_2. *ACS Nano* **4**(5), 2695 (2010).
25. M. Boukhicha, M. Calandra, M.A. Measson, O. Lancry, and A. Shukla: Anharmonic phonons in few-layer MoS_2: Raman spectroscopy of ultralow energy compression and shear modes. *Phys. Rev. B* **87**, 195316 (2013).
26. A. Rose: Recombination processes in insulators and semiconductors. *Phys. Rev.* **97**(2), 322 (1955).
27. N. Perea-López, A.L. Elías, A. Berkdemir, A. Castro-Beltran, H.R. Gutiérrez, S. Feng, R. Lv, T. Hayashi, F. López-Urías, S. Ghosh, B. Muchharla, S. Talapatra, H. Terrones, and M. Terrones: Photosensor device based on few-layered WS_2 films. *Adv. Funct. Mater.* **23**, 5511 (2013).
28. S. Kundu, S. Ghosh, M. Fralaide, T.N. Narayanan, V.K. Pillai, and S. Talapatra: Fractional photo-current dependence of graphene quantum dots prepared from carbon nanotubes. *Phys. Chem. Chem. Phys.* **17**, 24566 (2015).
29. K.K. Chi: *Dielectric Phenomena in Solids* (Academic Press, Burlington, 2004).
30. N.F. Mott and E. Davis: *Electronic Processes in Non-crystalline Materials* (Oxford University Press, London, 1971).
31. N. Kushwaha, V.S. Kushwaha, R.K. Shukla, and A. Kumar: Determination of energy of defect centers in a-$Se_{78}Ge_{22}$ thin films. *Philos. Mag. Lett.* **86**, 691 (2006).
32. N.A. Bakr: Anomalous photoconductive transport properties of As_2Se_3 films. *Egypt. J. Sol.* **25**, 13 (2002).
33. V. Klee, E. Preciado, D. Barroso, A.E. Nguyen, C. Lee, K.J. Erickson, M. Triplett, B. Davis, I-H. Lu, S. Bobek, J. McKinley, J.P. Martinez, J. Mann, A.A. Talin, L. Bartels, and F. Léonard: Superlinear composition-dependent photocurrent in CVD-grown monolayer $MoS_{2(1-x)}Se_{2x}$ alloy devices. *Nano Lett.* **15**, 2612 (2015).
34. H. Qiu, L. Pan, Z. Yao, J. Li, Y. Shi, and X. Wang: Electrical characterization of back-gated bi-layer MoS_2 field-effect transistors and the effect of ambient on their performances. *Appl. Phys. Lett.* **100**, 123104 (2012).
35. W. Park, J. Park, J. Jang, H. Lee, H. Jeong, K. Cho, S. Hong, and T. Lee: Oxygen environmental and passivation effects on molybdenum disulfide field effect transistors. *Nanotechnology* **24**, 095202 (2013).